Journal of CO_2 Utilization 33 (2019) 121–130

Contents lists available at ScienceDirect

Journal of CO_2 Utilization

journal homepage: www.elsevier.com/locate/jcou

Combining CO_2 conversion and N_2 fixation in a gliding arc plasmatron

Marleen Ramakers[a,*], Stijn Heijkers[a], Tom Tytgat[b], Silvia Lenaerts[b], Annemie Bogaerts[a]

[a] Research Group PLASMANT, Department of Chemistry, University of Antwerp, Universiteitsplein 1, 2610 Antwerp, Belgium
[b] Research Group DuEL, Department of Bioscience Engineering, University of Antwerp, Groenenborgerlaan 171, 2020 Antwerp, Belgium

ARTICLE INFO

Keywords:
CO_2 conversion
N_2 fixation
NOx
Gliding arc plasmatron
Plasma

ABSTRACT

Industry needs a flexible and efficient technology to convert CO_2 into useful products, which fits in the Carbon Capture and Utilization (CCU) philosophy. Plasma technology is intensively being investigated for this purpose. A promising candidate is the gliding arc plasmatron (GAP). Waste streams of CO_2 are often not pure and contain N_2 as important impurity. Therefore, in this paper we provide a detailed experimental and computational study of the combined CO_2 and N_2 conversion in a GAP. Is it possible to take advantage of the presence of N_2 in the mixture and to combine CO_2 conversion with N_2 fixation? Our experiments and simulations reveal that N_2 actively contributes to the process of CO_2 conversion, through its vibrational levels. In addition, NO and NO_2 are formed, with concentrations around 7000 ppm, which is slightly too low for valorization, but by improving the reactor design it must be possible to further increase their concentrations. Other NO-based molecules, in particular the strong greenhouse gas N_2O, are not formed in the GAP, which is an important result. We also compare our results with those obtained in other plasma reactors to clarify the differences in underlying plasma processes, and to demonstrate the superiority of the GAP.

1. Introduction

"A penny saved is a penny earned" is one important saying in industry. It is in this view that industry is looking for an easy and energy-efficient method to convert CO_2 from their waste streams. A technology intensively investigated for this purpose is based on plasma [1,2]. Plasma is created by applying electric power to a gas, causing breakdown of the gas into ions and electrons. It is thus a (partially) ionized gas, consisting of molecules, but also a large number of other species, such as various radicals, ions, excited species, and electrons. This makes plasma a highly reactive cocktail, useful for many applications [1,3]. The major advantage of plasma is that mainly the electrons are heated by the applied power, because of their small mass, and the energetic electrons can activate the gas by electron impact excitation, ionization, and dissociation, creating reactive species that can easily form new molecules. In this way, the gas as a whole does not have to be heated. Furthermore, owing to the fact that plasma can be switched on and off very easily, this technique also has great potential to store intermittent renewable energy, like solar and wind [2].

A very promising candidate for plasma-based CO_2 conversion is the gliding arc plasmatron (GAP). This is a three-dimensional gliding arc reactor [4,5]. A gliding arc (GA) plasma is created by applying a potential difference between two electrodes (cathode and anode), and typically moves (or glides) along these electrodes as a result of a gas flow. The GAP is a non-thermal plasma with different electron, and likely different vibrational, rotational and translational temperatures [6–8]. In the GAP under study here, the cathode forms the reactor body, while the reactor outlet is at anode potential. The gas enters through 6 tangential inlets so that a vortex flow is obtained. This stabilizes the arc plasma in the center of the reactor and part of the gas flow is actually forced to go through the plasma, while only limited heat loss occurs to the reactor walls. Note that the plasma column is actually not just convected by the gas flow, but moves slower than the gas flow surrounding the plasma column [9,10]. The splitting of pure CO_2 and the dry reforming of methane (DRM) have already been investigated in this GAP [4,5,11], as well as in similar designs [12–20], and showed very promising results in terms of energy efficiency (i.e. up to 46% for pure CO_2 splitting and up to 67% for DRM). However, most industrial gas flows contain impurities, or even large gas admixtures, and it is often economically not feasible to separate them from the gas stream [21]. Aiming for the industrial implementation of this technology, it is crucial to study the effect of these impurities on the CO_2 conversion and on the formation of byproducts.

Most often, N_2 is the main compound in gas effluents [22]. Therefore, we study in this paper the effect of N_2 on the plasma chemistry of CO_2 conversion. We have performed experiments in a broad range of N_2

* Corresponding author.
E-mail address: marleen.ramakers@uantwerpen.be (M. Ramakers).

https://doi.org/10.1016/j.jcou.2019.05.015
Received 7 March 2019; Received in revised form 1 May 2019; Accepted 10 May 2019

concentration to find out how it affects the CO_2 conversion, as well as the energy cost and energy efficiency. Furthermore, we analyzed which useful or harmful byproducts are formed. This is specifically interesting to find out whether purification is needed and whether pre- or post-purification steps would economically be most viable. Besides that, we also evaluate for the first time whether a mixture of CO_2 and N_2 could be a starting point for combined CO_2 conversion and N_2 fixation, i.e., the conversion of N_2 molecules into simple nitrogen compounds, that form the building blocks for life on Earth [23,24]. If sustainable electricity can be utilized for the plasma generation and further conversion of NOx into NH_3 can be realized, this can offer opportunities as a green alternative for the Haber-Bosch process [24,25] and more in general for N_2 fixation. It must be realized that the reaction products of the combined CO_2-N_2 conversion (CO and NOx) require separation or further oxidation steps to be used for fuel and fertilizer. Hence, this research is still on the fundamental level, and more research will be needed to bring it to real application. Finally, we have also performed chemical reaction simulations to unravel the underlying reaction pathways of CO_2 conversion in the presence of N_2, as well as of the byproduct formation.

To our knowledge, such a comprehensive experimental and computational study for the addition of N_2 to CO_2 in a GAP has never been performed. In addition, only a few papers have reported on the effect of N_2 on CO_2 conversion in other types of plasmas [16,26–28]. However, except in the paper by Snoeckx et al. [28], a detailed analysis of the byproduct formation in this mixture was never performed, which is of course crucial for practical applications. Furthermore, Snoeckx et al. [28] carried out this analysis for a dielectric barrier discharge (DBD), which has completely different plasma properties than a GAP [2]. The latter clearly affects the plasma chemistry, and thus the CO_2 conversion and byproduct formation. This will also be illustrated in this paper.

2. Description of the experiments

2.1. Gliding arc setup

The experiments were performed with a gliding arc plasmatron (GAP), which was developed at Drexel University by Nunnally et al. [4] and was previously described in detail [5]. A schematic picture of the GAP is shown in Fig. 1. The cathode (reactor body) has a length of 10.20 mm and a diameter of 17.50 mm, while the anode has a length of 16.30 mm and a diameter of 7.08 mm. These dimensions give rise to a reactor volume of 6.22 cm^3, but the arc volume is only about 0.13 cm^3. Indeed, it takes place only in the center of the reactor, thereby isolating the reactor walls from the hot plasma. A photograph and diagram of the entire experimental system is shown in Fig. 2.

Mass Flow Controllers (Bronkhorst) were used to insert CO_2 and N_2 into the GAP. The total flow rate was kept constant at 10 L/min. The N_2 concentration was varied between 5 and 95%. The reactor was powered by a DC current source type power supply. The plasma voltage and current were measured by a high-voltage probe (Tektronix P6015A) and a current sense resistor of 6 Ω, respectively. The electrical signals were sampled by a two-channel digital storage oscilloscope (Tektronix TDS2012C). The current was set at 0.23 A. The plasma power was calculated as the product of the plasma voltage and current over a certain time. All the experiments were performed three times. Subsequently, a propagation of uncertainty was applied to the results, to calculate the error bars.

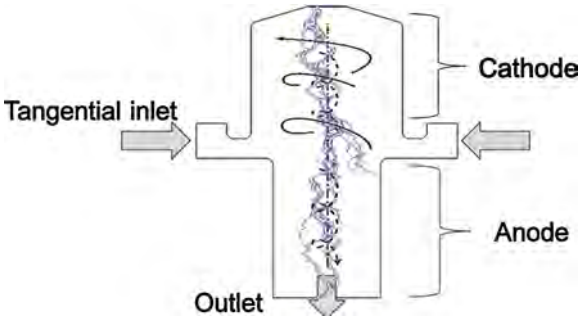

Fig. 1. Schematic picture of the gliding arc plasmatron in reverse vortex flow configuration. Both the forward and reverse vortex flows are indicated (with full and dashed spirals, respectively). This vortex flow configuration stabilizes the arc discharge (indicated in purple) in the center of the reactor and forces the reverse gas flow to go through the plasma.

2.2. Product analysis

The output gas composition is analyzed with three different gas analysis techniques: gas chromatography (GC) [5], Fourier Transform Infrared spectroscopy (FTIR) [28] and Quantum Cascade Laser (QCL) technology. The feed and main product gases (CO_2, N_2, CO, O_2) were analyzed by a three-channel compact gas chromatograph (CGC) from Interscience. Besides CO and O_2, some other products, like O_3 and NOx compounds (i.e., NO, NO_2, N_2O, N_2O_3 and N_2O_5) can be formed. We used a Nicolet 380 Fourier-Transform Infrared (FTIR) spectrometer (Thermo Fischer Scientific, Waltham, MA) and a CT5800 Analyzer (Emerson, Stirling, UK) based on Quantum Cascade Laser (QCL) technology to qualitatively and quantitatively analyze these products, respectively. These techniques, as well as the associated formulas to calculate the conversion, energy cost and energy efficiency, are described in detail in the Supplementary Information (Suppl. Info.).

3. Description of the model

The model used to simulate the chemical reactions in the GAP, is a 0D chemical kinetics model. It solves a set of conservation equations (Eq. 1) for all individual species included in the model:

$$\frac{dn_i}{dt} = \sum_j [(a_{ij}^R - a_{ij}^L)k_j \prod_{lj} n_{lj}] \quad (1)$$

n_i is the density of species i, a_{ij}^R and a_{ij}^L are the stoichiometric coefficients of the species i on the right and left hand side of the reaction j, respectively, n_{lj} is the density of the species l on the left side of reaction j, and k_j is the reaction rate coefficient of reaction j. For example, for the jth reaction A + B → C + D, the conservation equation for the density of species B is $\frac{dn_B}{dt} = (0-1)k_j n_A n_B$.

An extensive chemistry set, containing 18180 reactions and 134 species, is included in the model. The species interact with each other through electron impact reactions, electron-ion recombination, ion-ion, ion-neutral and neutral-neutral reactions, as well as vibration-translation (VT) and vibration-vibration (VV) relaxation. More information on these reactions and the list of species, as well as more details on the model, can be found in the Suppl. Info., including the GAP geometry as treated in the 0D model (Figure S1).

4. Results and discussion

4.1. CO_2 conversion, energy cost and energy efficiency

Fig. 3(a) shows that the absolute CO_2 conversion rises from 5 to 18% with increasing fraction of N_2 in the mixture. Hence, N_2 helps to convert CO_2, by the transfer of vibrational energy, as explained in section 'Simulation results' below. Indeed, CO_2 conversion in a GAP is most effective through the vibrational levels [5,29], and the N_2 vibrational levels help to populate these CO_2 vibrational levels. The same mechanism was also found for a microwave (MW) plasma [26], while in a DBD plasma, another mechanism is more prominent, i.e., energy transfer from the electronically excited N_2 molecules [28].

The effective CO_2 conversion is obtained by accounting for the initial fraction of CO_2 in the mixture (see Eq. (2) in the Suppl. Info.). Until

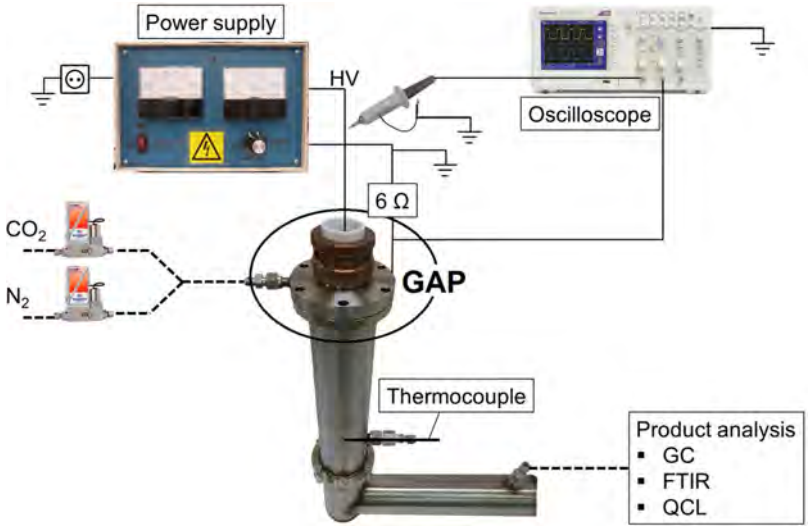

Fig. 2. The plasma in the gliding arc plasmatron (GAP) is initiated by applying a high voltage over two electrodes with a power supply. The setup is completed by Mass Flow Controllers for gas input and measuring equipment, i.e., electrical (oscilloscope), temperature (thermocouple) and product analysis.

a N_2 fraction of 50%, the effective conversion only slightly decreases, while above 50%, the effective conversion drops quite fast from 5 to 1% (see Fig. 3(b)). Thus, at N_2 fractions below 50%, the increase in absolute CO_2 conversion can more or less compensate for the lower CO_2 concentration in the mixture, but at higher N_2 fractions, this is not true anymore. Indeed, not all the energy of the vibrationally excited N_2 is transferred into CO_2 dissociation, and part of it also remains stored in the N_2 vibrational levels or gets lost by collisions with ground state molecules (so-called VT relaxation). Thus, at higher N_2 fractions in the mixture, a larger portion of the applied power is used to activate the N_2 molecules, without converting all this energy into CO_2 dissociation.

The energy cost of CO_2 conversion is calculated with equation (4) in the Suppl. Info., and is shown in Fig. 3(c). Until a N_2 fraction of 70%, the energy cost is about 40 kJ/L (or 10 eV/molec). At higher N_2 fractions, it rises dramatically to 210 kJ/L (or 52.5 eV/molec). The energy efficiency of CO_2 conversion (see Fig. 3(d)) more or less follows the trend of the effective CO_2 conversion, since it is approximately proportional to it. The fact that it does not exhibit exactly the same trend is due to a small drop in specific energy input (SEI) upon N_2 addition (see Figure S3 in the Suppl. Info.), as the energy efficiency is inversely proportional to the SEI (see equation (5) in the Suppl. Info.). The energy efficiency remains more or less constant around 28% until 50% N_2, after which it decreases rapidly to a value of 5%. Thus, upon increasing N_2 fraction, more energy is consumed by the N_2 molecules, which cannot be used anymore for CO_2 conversion. We can thus conclude that up to 50%, N_2 has little effect on the effective (i.e., overall) CO_2

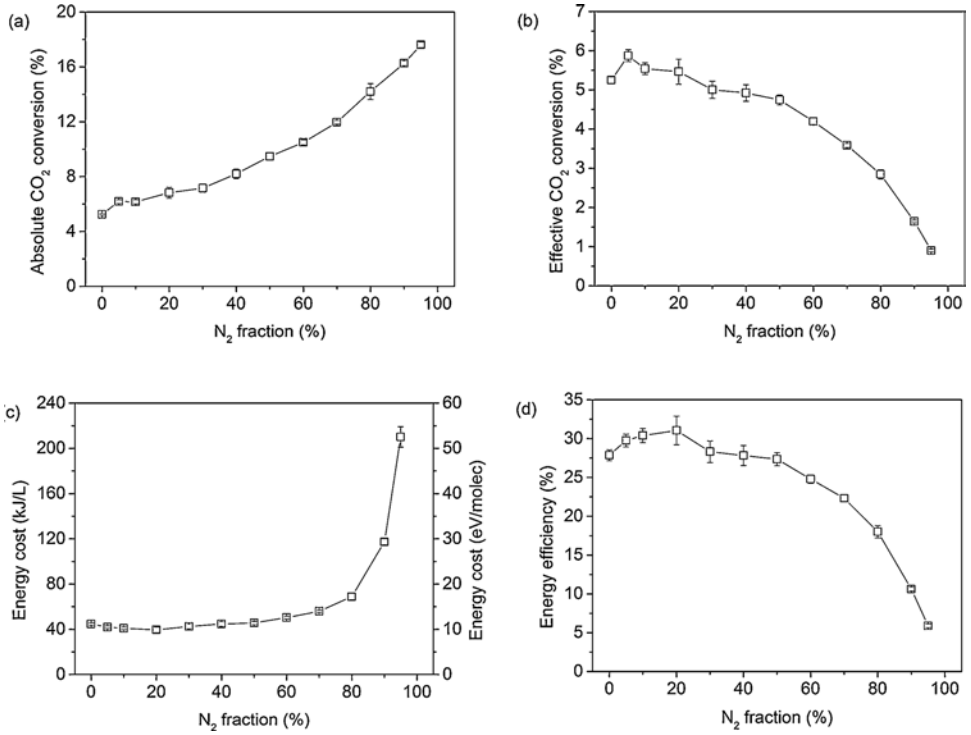

Fig. 3. Absolute (a) and effective (b) CO_2 conversion, energy cost (c) and energy efficiency (d), as a function of N_2 fraction, at a total flow rate of 10 L/min and a plasma power of 350 W. The error bars are included in the graphs, but are sometimes too small to be visible.

conversion, its energy cost and energy efficiency. In this respect, there is no need to separate N_2 from CO_2 in waste streams containing at maximum 50% N_2.

The energy cost and energy efficiency reached in our GAP are very good compared to other plasma reactors, i.e., DBD and MW plasma [26,28]. This is clearly demonstrated from Figure S4 in the Suppl. Info., where the energy efficiency is plotted against CO_2 conversion in GAP, DBD and MW plasma. The best energy efficiency is reached in our GAP, but for the CO_2 conversion, there is still room for improvement, and the MW plasma reaches higher conversion. Nevertheless, the experiments with MW plasma were performed at reduced pressure (2660 Pa), while the GAP and DBD both operate at atmospheric pressure. If the pressure in the MW plasma would be increased, the conversion and energy efficiency would drop [2,30,31], and in addition the plasma would become less stable [2,31]. When operating at reduced pressure, the energy cost of pumping should also be accounted for, and this would lower the overall energy efficiency (not yet included in Figure S4). For industrial application of this technology, it would be beneficial to work at atmospheric pressure or higher.

4.2. Analysis of the byproducts - NOx concentrations

Not only conversion and energy efficiency are important for evaluation of this technology, but also the formation of byproducts. We used FTIR as qualitative analysis method for the byproducts, i.e., O_3 and NOx compounds (NO, NO_2, N_2O, N_2O_3 and N_2O_5). Note that in terms of N_2 fixation, the NOx compounds are products rather than byproducts. However, as the main goal of the research was CO_2 conversion (in the presence of N_2 from a waste stream), the NOx compounds can be considered as byproducts, which can be of added value as well, if produced in sufficient amounts. The components that could be clearly distinguished from the FTIR-spectrum are CO, NO and NO_2. There were no signals visible for other components, like O_3, N_2O, N_2O_3 and N_2O_5. The influence of N_2 fraction on the NO and NO_2 concentration in arbitrary units is plotted in Figure S5 of the Suppl. Info. To quantitatively analyze the NOx compounds, we used a CT5800 Analyzer based on Quantum Cascade Laser (QCL) technology. The QCL could not detect any N_2O, in agreement with the FTIR analysis, indicating that the concentration of N_2O was never higher than 1 ppm. The concentrations of NO and NO_2 as well as the sum of both, are plotted in Fig. 4 as a function of N_2 fraction. The error bars are too small to be visible, as they were typically below 1% of the actual concentrations, but the actual values of the concentrations, along with their absolute errors, are listed in Table S4 of the Suppl. Info. All curves show a maximum around 50–70 % N_2. This is expected, because in this range, both CO_2 and N_2 split into the reactive species needed for NO and NO_2 formation. At very low or high N_2 fractions, either N_2 or CO_2 will act as limiting reactant. The fact that the maximum NO concentration is reached around 60–70% N_2 indicates that CO_2 dissociation occurs easier than N_2 dissociation, which is explained by the C═O vs N≡N bond dissociation energy (i.e., 749 kJ/mol vs 946 kJ/mol). The maximum NO_2 concentration is reached at 50% N_2, which is lower than for the maximum NO concentration. This is expected, because more CO_2 is needed, and thus less N_2, for the further oxidation of NO to NO_2 (see Fig. 6). Looking at the absolute values, the NO concentration is about 20 times higher than for NO_2, with maximum values of 6453 and 317 ppm, respectively.

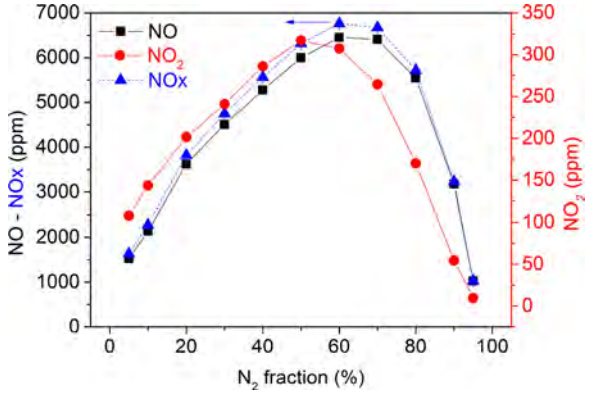

Fig. 4. NO (left axis), NO_2 (right axis) and total NOx (left axis) concentration as a function of N_2 fraction. The error bars are too small to be visible, as they were typically below 1% of the actual concentrations.

The highest total NOx concentration is 6761 ppm, reached at 60% N_2. Patil et al. reported the highest NOx formation in a pulsed power milli-scale classical (planar) gliding arc (GA) reactor [32,33] to be 2%, with 9470 ppm NO and 10,653 ppm NO_2 at 1 L/min and a 1/1 N_2/O_2 ratio. NO_2 formation from dry air in a classical GA was investigated by Bo et al. [34] in the context of VOC decomposition, reaching a maximum NO_2 content of 6982 ppm. Compared to our reactor, the NO_2 concentration lies much higher in the abovementioned studies. The reason is the higher temperature in our GAP, which favors NO above NO_2 formation, as revealed by our computer simulations. Moreover, these studies were for NOx formation from N_2/O_2 as a starting mixture, where simply more O_2 is available to form NO_2, while in our case it depends on the CO_2 conversion. Indeed, we investigate the possibilities for NOx formation from CO_2/N_2 as starting mixture. If this is feasible, we do not only fixate N_2 but also convert CO_2 at the same time. In this way we accomplish two goals at once.

A possible downside, however, can be the more complicated separation of CO from the mixture, compared to pure CO_2 splitting. Nevertheless, some technologies are already available today for the purification of CO-containing streams with emphasis on CO/N_2 separation, such as cryogenic distillation and absorption [35]. However, the associated energy consumption of such an approach and/or the poor stability of the absorbents have led researchers to concentrate on adsorption technologies, which are currently under development. Examples of adsorbents are zeolites (particularly Zeolites X and Y), modified activated carbons (particularly via impregnation with copper), as well as metalorganic frameworks [35]. In another approach, the produced NOx could be catalytically converted into HNO_3 first. Subsequently, the CO can be separated in a similar way by for example pressure swing adsorption (PSA) as in the case of pure CO_2 splitting. Hence, for this approach, the catalytic conversion of NOx into HNO_3 represents an extra step for the separation. This should be taken into account when investigating the economic feasibility of the combined CO_2/N_2 conversion. However, this is outside the scope of the present study.

Plasma-based NOx formation from N_2/O_2 mixtures has also been studied in a large number of other plasma types [32,33,36–49]. An overview of the measured values for NOx yield and energy consumption is given in Table 1. Note that only in our work and that of Snoeckx et al. [28] the starting mixture is CO_2/N_2, whereas in all other cases it is N_2/O_2.

The NOx yield reported in literature ranges from 0.06–14 %, while the energy consumption ranges from 0.3–1638 MJ/mol NOx. Thus, the GAP seems to perform at the lower limit for the NOx yield, but it performs quite well in terms of energy consumption, with a moderate value around 7 MJ/mol NOx. To make a fair comparison, however, we have to take into account that our starting mixture is CO_2/N_2. Therefore, the NOx yield is limited by the CO_2 conversion, which supplies the oxygen for NOx formation. In addition, this also affects the energy consumption, since part of the energy input is also used for CO_2 conversion and not only for NOx production. The real energy consumption for NOx formation in the GAP will thus be lower than 7 MJ/mol NOx.

For a DBD reactor with [32,42] and without catalyst [28], the NOx yield is lower with considerably higher energy consumption than for microwave (MW) and gliding arc (GA) discharges (although the energy consumption of 442 MJ/mol NOx from ref [28]. is again obtained for a

Table 1
Overview of measured values for NOx yield and energy consumption for various plasma types[a].

plasma type	NOx concentration	energy consumption	ref
gliding arc plasmatron (GAP) (*)	0.7 % NOx	7.02 MJ/mol NOx	this work
DBD (*)	0.06 % NOx	442 MJ/mol NOx	28
DBD with y-Al_2O_3 catalyst	0.5 % NOx	18 MJ/mol NOx	32,42
milliscale GA with pulsed power	2 % NOx	7.2 MJ/mol NOx	32,33
milliscale GA with pulsed power	0.8 % NOx	2.8 MJ/mol NOx	32,33
pulsed arc discharge	–	10.6 MJ/mol NOx	36
plasma arc jet	6.5 % NO	4.0 MJ/mol NO	37
laser-produced plasma	–	8.96 MJ/mol NO	38
exploding water jet discharge	1 % NOx	47.2 MJ/mol NOx	39
negative pulsed corona discharge	–	1638 MJ/mol NOx	40
positive pulsed corona discharge	–	1060 MJ/mol NOx	40
spark discharge	–	20.2 MJ/mol NOx	40
spark discharge	1 % NOx	2.41 MJ/mol NOx	41
MW discharge with MoO_3 catalyst	6 % NO	0.84 MJ/mol NO	43
pulsed MW discharge	6 % NO	0.60 MJ/mol NO	44
MW discharge with magnetic field	14 % NO	0.30 MJ/mol NO	45
MW discharge	0.6 % NOx	4.05 MJ/mol NOx	46
shielded sliding discharge	0.1 % NOx	15.4 MJ/mol NOx	47
electric arc (original Birkeland-Eyde process)	1 – 2 % NO	2.41 MJ/mol NO	48
electric arc with water injection	4.7 % NO	3.50 MJ/mol NO	49

[a]In some references, the NOx yield was not mentioned, and only the energy consumption was mentioned.
(*) CO_2/N_2 as starting mixture.

CO_2/N_2 mixture, explaining the higher value). The reason is that MW and GA plasmas are characterized by a reduced electric field (i.e., ratio of electric field over gas number density) between 5 and 100 Td, where the dominant electron-induced process is vibrational excitation of N_2, [24] similar as for CO_2 [2]. Thus, in GA and MW discharges large amounts of vibrationally excited N_2 molecules are present, which provide more energy-efficient N_2 dissociation. DBDs are characterized by higher reduced electric fields, above 100–200 Td, where mostly electronically excited species are involved in NOx production, which is thus limited by the higher energy cost for the formation of these species (see more details below).

Comparing our results with those of the milliscale GA from Patil et al. [32,33], their NOx yield is more than twice as high, while the energy consumption is quite similar. However, we produce NOx from CO_2/N_2 instead of N_2/O_2, and part of the energy is consumed by CO_2, as explained above. We can conclude that NOx production from a CO_2/N_2 mixture in a GAP is worth investigating further, since it has similar energy consumption than starting from an N_2/O_2 mixture and it can solve two problems at the same time. Some ways to increase the NOx yield in our GAP are suggested below.

The best results up to now were obtained in MW plasmas [43–45] but only at reduced pressure, which requires pumping, making it less attractive for industrial implementation, and it should be accounted for in the calculation of the energy consumption, which was not the case for the values in Table 1. Unfortunately, the cost for pumping was not mentioned in these references, so we cannot make a fair comparison between these and our data, which were obtained at atmospheric pressure.

To make the process effective for N_2 fixation, the NOx concentration should increase to about 1% [23,50]. Indeed, such low concentrations can already provide high concentrations of $HNO_3$50]. The CO_2 conversion in our GAP is limited to 8–18 %, due to the limited amount of gas passing through the actual arc plasma [5,11,51]. If this fraction can be enhanced by optimizing the reactor design or the gas inlet system, it would yield higher CO_2 conversions, and thus the NOx concentration could also rise further. Previously we found that lowering the flow rate also increases the CO_2 conversion [5]. However, a minimum flow rate of 10 L/min is necessary for obtaining a stable plasma, because of the need of a good vortex flow pattern. Such a calculated vortex flow pattern was presented in the SI (Fig. 6) of reference [5]. From previous calculations we know that the fraction of gas passing through the arc is 15% [11], meaning that the conversion inside the arc is about 71%. Hence, we have to increase the fraction of gas passing through the arc up to minimum 22%, which results in a CO_2 conversion of 16%, if we want to reach a NOx concentration above 1% (see more details in the Suppl. Info.). A way to increase this fraction is by decreasing the radius of one or more tangential inlets in order to create a higher flow velocity so that more gas is forced into the central vortex. Besides this approach, we also want to change the cathode design to increase the electric field, which also increases the plasma production and arc stability. Dedicated fluid dynamics simulations are needed to evaluate these approaches, which is the subject of our future work.

The selectivity towards NO and NO_2 (see Eqs. (2) and (3)) are plotted as a function of N_2 fraction in Fig. 5.

$$NO\ selectivity\ (\%) = \frac{NO\ concentration}{concentration\ of\ (NO + NO_2)} \times 100\,\% \quad (2)$$

$$NO_2\ selectivity\ (\%) = \frac{NO_2\ concentration}{concentration\ of\ (NO + NO_2)} \times 100\,\% \quad (3)$$

The NO selectivity rises from 93 to 99% with increasing N_2 fraction, while the NO_2 selectivity decreases from 7 to 1%. These trends are similar as in Wang et al. [24] for NOx formation from a N_2/O_2 mixture in a milli-scale classical (planar) GA, but the absolute values are clearly

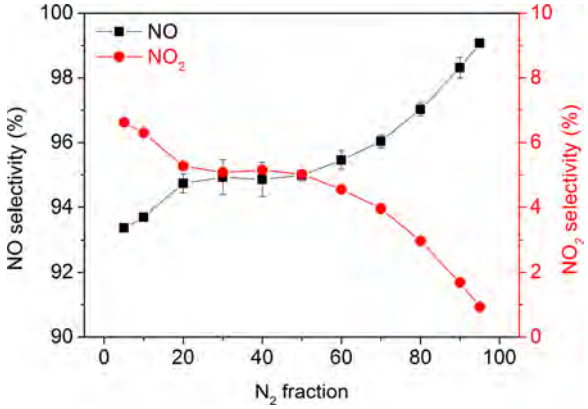

Fig. 5. NO (left axis) and NO_2 (right axis) selectivity as a function of N_2 fraction. The error bars are included in the graph, but for some conditions they are too small to be visible.

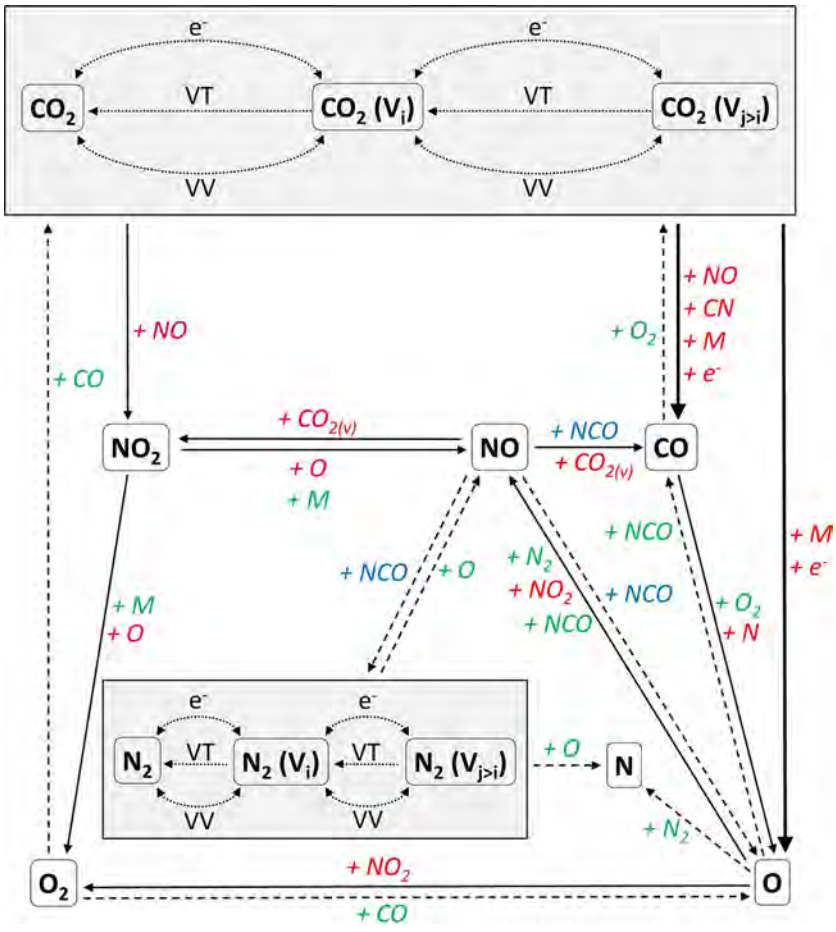

Fig. 6. Reaction pathways for the conversion of CO_2 and N_2 into CO, O, O_2, N, NO and NO_2, as predicted by the model. Both CO_2 and N_2 are easily excited from ground state to vibrational levels and vice versa (dotted lines). The color of the reactants indicates the time-integrated rate of their reaction (red $\geq 10^{17}\,cm^{-3}$; green $\geq 10^{16}\,cm^{-3}$; blue $\geq 10^{15}\,cm^{-3}$) while the thickness of the arrow lines corresponds to the total importance of the reactions (▬ < ▬ < ■).

different. Indeed, Wang et al. [24] obtained more or less equal selectivities of 50% for NO and NO_2, except at very high or low N_2 concentrations, while in our GAP the selectivity towards NO is much higher than towards NO_2. This is attributed to the much higher temperature in our GAP (i.e., nearly 3000 K [51], vs. 1000–1500 K in the classical GA [24]), favoring NO above NO_2, as well as the different starting mixture, and hence different reaction mechanisms for the formation of NO and NO_2, as explained in the 'Simulation results' section.

In fact, the separate NO and NO_2 concentrations are not so important, as NO can easily be oxidized into NO_2 after plasma, so it is the total NOx concentration that counts. When the NOx concentrations will still be a bit higher and thus effective for N_2 fixation, the NO/NO_2 mixture can be separated from the unconverted fraction by taking part in the Ostwald process, thereby producing nitric acid [50]. This can be used as precursor for the synthesis of more complex molecules, such as mineral fertilizers. In the industrial Ostwald process, NH_3 is first oxidized to NOx and then absorbed by H_2O to form HNO_3. The typical yield from NH_3 to NOx is about 98%. In our case, HNO_3 would also be made from NOx absorption by H_2O, but the yield from N_2 to NOx is considerably lower than in the industrial Ostwald process, so our process is by far not yet competitive with the Ostwald process. However, overall, producing HNO_3 from NH_3 is less sustainable, because the production of NH_3 is enormously energy intensive and produces a lot of CO_2. Hence, alternatives for the Haber-Bosch (HB) process must be investigated, and plasma technology is very promising in this respect, exactly because it can easily be combined with renewable energy, and it is thus a sustainable alternative, especially for distributed production. Furthermore, the energy efficiency is very good, due to the selective vibrational activation of the molecules. The potential of plasma technology was also recognized in a recent paper: "Nearly all nitric acid is manufactured by oxidation of NH_3 through the Ostwald process, but a more direct reaction of N_2 with O_2 might be practically feasible through further development of nonthermal plasma technology" [52].

Although several green technologies for NH_3 production from N_2 are being developed to replace the energy-intensive HB process [53–57], the goal of our plasma process is different: it is mainly used for CO_2 conversion, and by making use of a waste stream containing N_2, we can also produce NOx, which can be further converted to HNO_3, without producing NH_3 as an intermediate step. Hence, we believe our plasma process is a unique concept.

4.3. Underlying mechanisms as revealed by numerical simulations

We developed a chemical kinetics model to investigate the mechanisms of the combined CO_2 and N_2 conversion in our GAP (see brief explanation above and more details in the Suppl. Info.). The model has been validated against the experimental data for conversion, energy efficiency and NOx concentrations. In all cases, the trends and absolute values predicted by the model were in reasonable agreement with the experimental results, as illustrated in Figures S6 and S7 in the Suppl. Info. Indeed, on average the relative difference between calculated and experimental data was 5% for the CO_2 conversion, 27% for the N_2 conversion, 5% for the energy efficiency, 34% for the NO concentration, and 72% for the NO_2 concentration. The largest deviation was found for NO_2 concentration, but keeping in mind the complexity of the underlying chemistry, this is still reasonable. Therefore, we can use the model to predict the underlying mechanisms. In Figures S8, S10 and S12 in the Suppl. Info., we present the net time-integrated rates of the most important reactions for the loss and formation of CO_2, NO and NO_2, respectively. For additional insight, we also plotted the net contributions of these reactions in Figures S9, S11 and S13 in the Suppl. Info.

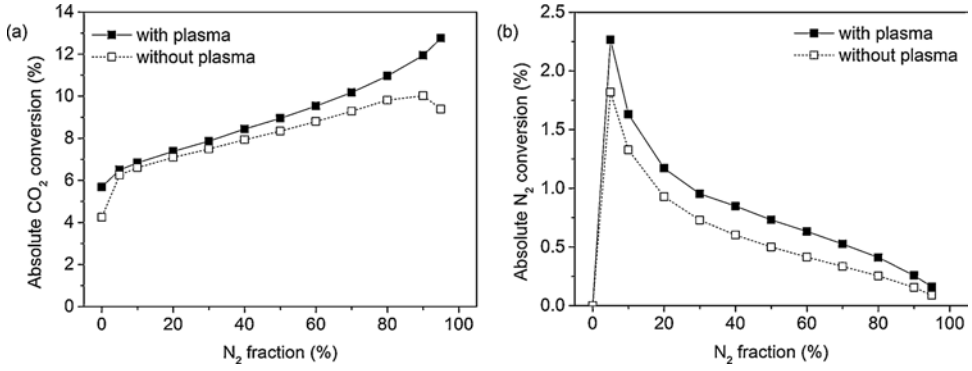

Fig. 7. Calculated absolute CO_2 (a) and N_2 (b) conversion in the GAP as a function of N_2 fraction in the mixture, comparing with plasma and without plasma (i.e., only thermal reactions, without electron impact reactions).

For pure CO_2 the most important loss mechanism is the reaction of vibrationally excited CO_2 with O atoms, see Figure S8(a). This agrees well with earlier model predictions [5]. However, as soon as N_2 is added, the reaction of vibrationally excited CO_2 with NO becomes dominant, with an overall contribution of 50–60 % (Figure S9). Other reactions, such as the collision of vibrationally excited CO_2 with CN or any molecule M in the plasma, and electron impact dissociation of both CO_2 ground state and vibrationally excited levels, also play a role, with contributions of 5–60 %, depending on the N_2 fraction (Figure S9). CO_2 formation is mainly caused by recombination of CO and O_2 (Figure S8(b)), with contributions up to 80% (Figure S9). To prevent this recombination and thus enhance the CO_2 dissociation, we could separate O_2 from the mixture, e.g., by membrane technology or oxygen scavengers.

NO is initially formed upon reaction of vibrationally excited N_2 with O atoms, i.e., the so-called Zeldovich mechanism, in agreement with the dominant formation mechanisms in a milli-scale classical GA [24]. Subsequently, NO reacts with vibrational excited CO_2, forming CO and NO_2 (Figure S10). In return, the reaction of NO_2 with O atoms will further produce NO.

We summarize the most important reaction pathways in Fig. 6. Reactants are indicated in color according to the time-integrated rate of their reaction (red $\geq 10^{17}\,cm^{-3}$; green $\geq 10^{16}\,cm^{-3}$; blue $\geq 10^{15}\,cm^{-3}$), while the thickness of the arrow lines corresponds to the overall importance of the reaction. The most important reactions, ranked by importance based on the average time-integrated rates, are listed in Table S5 in the Suppl. Info.

Both CO_2 and N_2 are easily excited from ground state to vibrational levels, and vice versa, upon electron impact (de)excitation, vibration-vibration (VV) and vibration-translation (VT) relaxation. The vibrational distribution functions (VDFs) of both CO_2 and N_2 are plotted in Figure S14. Overall, the VDF of both molecules is thermal, with a vibrational temperature of 3174 K and 3333 K for CO_2 and N_2, respectively (Figure S15), which is more or less equal to the gas temperature (3140 K). We should be able to increase the energy efficiency of CO_2 conversion and N_2 fixation if the VDFs of both CO_2 and N_2 would be more non-thermal, with higher populations of the higher vibrational level [5,29]. To realize this, the temperature in the arc should be reduced, so that VT relaxation, which depopulates the vibrational levels, can be reduced. On the other hand, the vibrational levels in our GAP are clearly more populated than in other types of plasmas, such as a DBD, where the VDF dramatically drops for the higher vibrational levels [58–60]. This explains why the CO_2 conversion and N_2 fixation are quite energy efficient, compared to other commonly studied plasma types (see Figure S4 in the Suppl. Info. and Table 1 above).

CO_2 is mainly converted into CO and O (right arrows in the figure), and it also helps in producing NO_2 upon reaction with NO. CO is in turn mainly converted into O by reaction with N or O_2. The N_2 molecules are activated by electron impact vibrational excitation (see Fig. 6), lowering their energy barriers for chemical reaction with O atoms into NO formation. NO reacts further into NO_2, mainly by reaction with vibrationally excited CO_2. Vice versa, NO_2 also stimulates the formation of NO, by reaction with O atoms or any molecule (M) in the plasma. The fact that the most important loss mechanism of NO_2 is the most important formation mechanism of NO, and vice versa (Figure S10 and S12), shows that they are easily converted into each other. Still, the selectivity of NO is much higher in our GAP than that of NO_2. Indeed, NO is also formed upon reaction of O atoms with vibrationally excited N_2 (Zeldovich mechanism; cf. above) and with NCO, which have no reverse reaction (Figure S10). Thus, by comparing the sum of the time-integrated formation and loss rates, the resulting concentration of NO is 20 times higher than that of NO_2 (see Fig. 5), which explains the higher NO selectivity.

We can in general conclude from Fig. 6 that the NOx molecules are mainly formed through reactions with O atoms. So to enhance the NOx production, we have to stimulate the formation of O atoms, and thus the CO_2 conversion, e.g., by improving the reactor design to enhance the fraction of gas passing through the arc.

Finally, as mentioned above, the gas temperature in the GAP is fairly high (around 3000 K), and the VDFs of both CO_2 and N_2 are thermal (see Figure S14), and thermal reactions are important for the CO_2 and N_2 conversion at this high temperature. Nevertheless, the CO_2 and N_2 molecules are first activated by electron impact excitation. To show the contribution of plasma in the CO_2 and N_2 conversion, we plot in Fig. 7 the calculated absolute CO_2 and N_2 conversion in the GAP as a function of N_2 fraction in the mixture, comparing with plasma and without plasma (i.e., only thermal reactions, without electron impact reactions). It is clear that, because of the high temperature, thermal reactions are indeed most important. Indeed, although the VDF is thermal, the higher vibrational levels are still sufficiently populated at this high temperature, to cause dissociation. Nevertheless, the conversion in case of plasma is still somewhat higher than the pure thermal conversion, especially at higher N_2 fractions, because the electron impact reactions create extra reactive species for the thermal reactions.

4.4. Comparison of GAP with DBD

As mentioned in the Introduction, Snoeckx et al. [28] have also analyzed the byproducts formed in a CO_2/N_2 mixture, but for a DBD plasma, which has completely different plasma properties than a GAP, [2] hence affecting the plasma chemistry. Therefore, we compare here both plasma reactors in terms of conversion efficiency and byproduct formation, at typical GAP and DBD conditions, i.e., a specific energy input (SEI) of around 2 kJ/L and 12 kJ/L, respectively. These values originate from a plasma power of 350 W and a total flow rate of 10 L/min for the GAP, while the plasma power and total flow rate in the DBD reactor are around 120 W and 611 mL/min, respectively. Note that we cannot compare the results in the GAP and DBD at the same SEI,

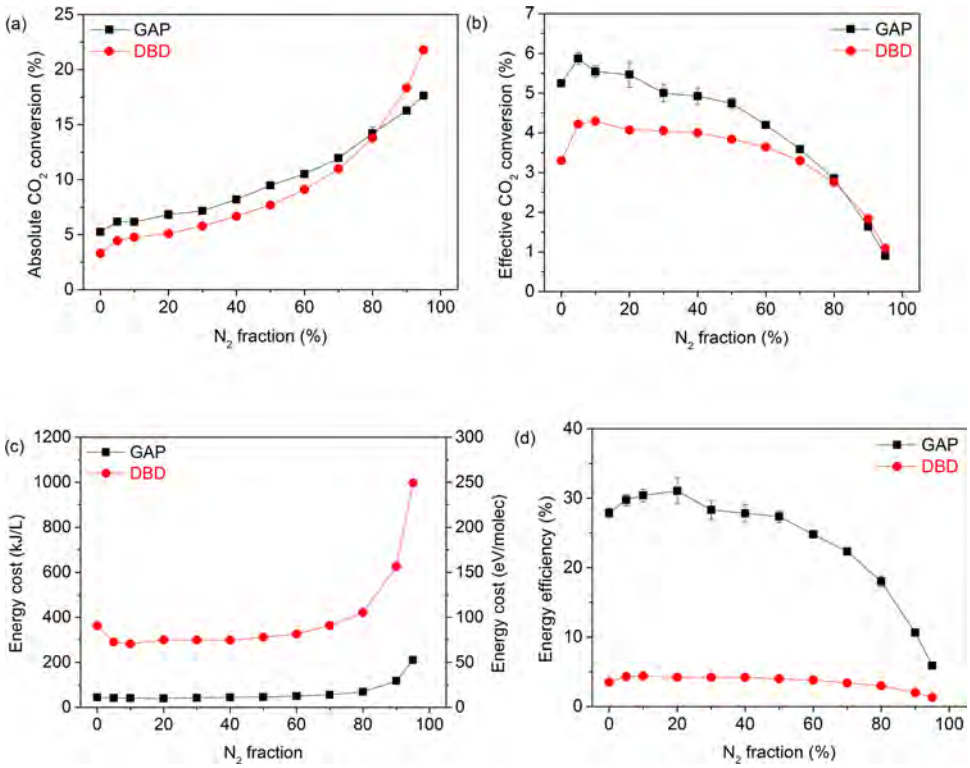

Fig. 8. Absolute (a) and effective (b) CO_2 conversion, energy cost (c) and energy efficiency (d), as a function of N_2 fraction, both for the GAP and DBD. The error bars are included in the graphs, but are sometimes too small to be visible.

because the flow rate in the GAP is much higher, which is necessary to obtain a good vortex flow pattern, while such a high flow rate would result in very small residence times, and thus virtually no conversion, in a DBD. However, this difference in flow rate (and power) must be accounted for when we compare the results in the GAP and DBD.

4.4.1. *CO_2 conversion, energy cost and energy efficiency*

In Fig. 8(a), the absolute CO_2 conversion is plotted for both plasma reactors as a function of N_2 fraction. The GAP shows a slightly more than linear trend with increasing N_2 fraction, while the trend of the DBD is more exponential. The absolute values in the GAP are somewhat higher than in the DBD, even at much lower SEI (cf. above). Only at the highest N_2 fractions, the values are higher in the DBD (i.e., 22% vs 18%). Thus, in general the CO_2 conversion is higher in the GAP, but the addition of large amounts of N_2 in a DBD enhances the CO_2 conversion more compared to in a GAP. To explain this, we should compare the main dissociation mechanisms of CO_2 in DBD and GAP. In a DBD the main dissociation mechanism is electron impact dissociation of ground state CO_2, but with increasing N_2 fraction, the reaction of CO_2 with metastable N_2 molecules becomes more important, and is the most important dissociation mechanism above 70% N_2 addition. [28] In our GAP, the reaction of vibrationally excited CO_2 with dissociated N_2 products, i.e., mainly NO but also CN (Figure S8(a)), is the most important CO_2 dissociation process. The reaction with NO is dominant up to 80% N_2, while above 80%, the reaction with CN becomes most important, but its absolute rate is quite low (Figure S8(a)), because CN also needs C to be formed, which is low at low CO_2 fractions. Thus, at high N_2 fractions, the contribution of N_2 is more important in a DBD than in a GAP, explaining why the GAP and DBD curves intersect at ca. 80% N_2. As is clear from Fig. 8(b), the effective CO_2 conversion is higher in the GAP than in the DBD, except again at N_2 fractions above 80%, where the values are comparable. The energy cost in the DBD is on average 6 times higher than in the GAP; see Fig. 8(c). Indeed, the effective conversion is slightly lower, but the SEI in the plasma is much higher (12 kJ/L vs 2 kJ/L). Thus, our GAP is much more promising than a DBD for plasma-based CO_2 conversion [2]. The energy efficiency in both plasma reactors decreases with increasing N_2 fraction (see Fig. 8(d)). In addition, the energy efficiency is 7 times higher in the GAP than in the DBD, for N_2 fractions up to 50%, i.e., around 27–31 % for the GAP vs. 4% for the DBD. At N_2 fractions above 50%, the difference becomes smaller, as the values drop to 5.9% for the GAP and 1.3% for the DBD, at 95% N_2. Indeed, in the DBD, the main mechanism of CO_2 dissociation is electron impact dissociation from ground state CO_2 molecules [28], which requires much more energy than the vibrational pathway in the GAP, this explains the better energy efficiency in the GAP than in the DBD.

4.4.2. *Byproduct formation*

We can conclude from above that the GAP is definitely superior for CO_2 conversion in the presence of N_2, in terms of conversion efficiency. However, for industrial application, also the formation of byproducts is important. The concentrations of NO and NO_2, obtained in the GAP and DBD are compared in Fig. 9, as a function of N_2 fraction in the mixture.

Both the NO and NO_2 concentrations follow the same trend as a function of N_2 fraction in the GAP and DBD, with a maximum around 50–60% N_2. This is striking, as the formation mechanisms in both plasma types are quite different (see ref. [28]). However, the reason is that in both mechanisms important in GAP and DBD, both N_2 and CO_2 first have to be split into reactive species needed for NO formation, and this condition is fulfilled most when both N_2 and CO_2 are present in somewhat equal amounts. Indeed, in both GAP and DBD, when there is mainly N_2 in the mixture, CO_2 will be the limiting reactant for NO formation, while in case of mainly CO_2 in the mixture, N_2 will be the limiting reactant.

However, the NO and NO_2 concentrations are more than 10 times and about 6 times higher in the GAP than in the DBD. This can only partly be explained by the higher effective CO_2 conversion (Fig. 8(b)). Indeed, the N_2 dissociation – also needed for NOx formation – is a factor 4 higher in the GAP than in the DBD (i.e., 4% vs. 1%). In addition, the selectivity towards NO and NO_2 is significantly higher in the GAP than

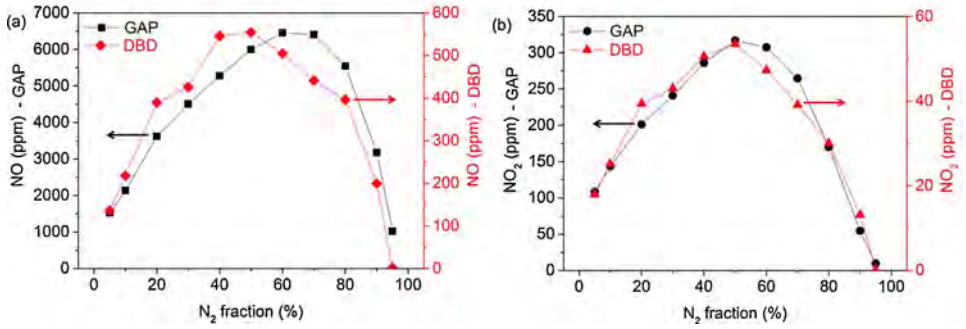

Fig. 9. NO (a) and NO_2 (b) concentration as a function of N_2 fraction, both for the GAP and DBD. The error bars are included in the graphs, but are too small to be visible.

in the DBD, where also other NOx compounds were formed [28].

It is indeed remarkable that in our GAP no N_2O, N_2O_3 and N_2O_5 could be detected, while they were clearly detected in the DBD, with the same measuring equipment (FTIR) [28]. Our simulation results also indicate NO and NO_2 as the major byproducts of CO_2 and N_2 conversion in the GAP, in agreement with our experiments, while N_2O (0.1–3 ppm), N_2O_3 (10^{-8} – 10^{-7} ppm), N_2O_4 (10^{-11} – 10^{-9} ppm) and N_2O_5 (10^{-12} – 10^{-10} ppm) have much lower concentrations (Figure S16 (a)). In comparison, in a DBD, next to NO and NO_2 also N_2O and N_2O_5 are formed in relatively high concentrations, i.e., calculated up to 115 ppm for NO, 34 ppm for NO_2, 55 ppm for N_2O, and even up to 1000 ppm for N_2O_5; see Figure S16(b) and also ref. [28]. The N_2O_3 and N_2O_4 concentrations are calculated to be much lower.

The reason we only detected NO and NO_2 in our experiments, while in the DBD also N_2O, N_2O_3 and N_2O_5 were detected, is attributed to the different plasma temperature. It is predicted to be around 3000 K inside the arc [51] in our GAP (for pure CO_2), which is too high to form N_2O, N_2O_3 and N_2O_5. Indeed, at higher temperatures the formation rates of these species increase but the loss rates are even higher (Figure S17), which results in lower net concentrations (Figure S16). On the other hand, a DBD operates around room temperature, yielding higher formation than loss rates (Figure S17), resulting in higher net concentrations (Figure S16). Furthermore, DBD plasmas are characterized by streamers, with short lifetime (order of 30 ns [61]), in which mainly electron impact reactions occur, but in between these streamers, NO_2 can interact with NO or NO_3 to form N_2O_3 and N_2O_5 respectively [28]. This is not the case in a GAP, because the arc is continuously stabilized in the center, explaining why only NO and NO_2 are detected in our experiments.

Taking into account that N_2O is a very potent greenhouse gas, with a global warming potential (GWP) of 298 $CO_{2,equivalent}$, it is highly beneficial that its concentration in the GAP does not exceed the detection limit of 1 ppm. After all, the production of N_2O would void the greenhouse gas mitigation potential of plasma technology if no denox purification step would be added.

Overall we can conclude that the GAP is far superior for CO_2 conversion in the presence of N_2 than the DBD, due to the higher conversion, but especially the absence of N_2O, N_2O_3, N_2O_5 formation, and the significantly higher energy efficiency.

5. Conclusions

We have investigated the effect of N_2 on CO_2 conversion in a GAP, by combining experiments and simulations. The addition of N_2 has a positive effect on the absolute CO_2 conversion up to 50%, while at higher N_2 fractions, the effective CO_2 conversion and energy efficiency drop. Our simulations reveal that the CO_2 conversion mainly proceeds through the vibrational levels, which are populated through collision with the N_2 vibrational levels. In addition, NO and NO_2 are formed in the CO_2/N_2 mixture, initiated by the reaction between N_2 vibrational levels and O atoms (so-called Zeldovich mechanism [24]).

Combining CO_2 and N_2 in a GAP thus can lead to combined CO_2 conversion and N_2 fixation. The highest amount of NOx obtained is 6761 ppm, which is still below the minimum threshold of 1% to make it effective for N_2 fixation. By improving our reactor and gas inlet design, we should be able to enhance the gas fraction that passes through the arc, and thus the CO_2 conversion and NOx production. This optimization will need dedicated fluid dynamics simulations, which are planned in our future work.

We compared the performance of our GAP with other plasma types. The best energy efficiency for CO_2 conversion is reached in our GAP, but the conversion itself needs further improvement. In terms of NOx production, the NOx yield is still quite low (attributed to the limited CO_2 conversion), but the energy consumption is reasonable compared to other plasma types, certainly if we take into account that our energy consumption also includes the cost for CO_2 conversion.

Finally, we made a more detailed comparison with a DBD, which is the only other work in literature where NOx production was also studied from a CO_2/N_2 mixture. The energy efficiency was 7 times higher in our GAP than in the DBD, next to a somewhat higher CO_2 conversion. Indeed, CO_2 dissociation in the GAP proceeds through vibrationally excited states, while in a DBD it occurs mainly by electronic excitation, which is less efficient [2]. Furthermore, our GAP only produces NO and NO_2, while N_2O, N_2O_3 and N_2O_5 are also formed in a DBD. Keeping in mind that N_2O is a very potent greenhouse gas, it is highly beneficial that its concentration in the GAP does not exceed the detection limit of 1 ppm. Overall, the GAP is superior for CO_2 conversion in the presence of N_2 compared to a DBD, due to its higher conversion, but especially the absence of N_2O, N_2O_3, N_2O_5 formation and the much higher energy efficiency.

Acknowledgements

We acknowledge financial support from the Fund for Scientific Research Flanders (FWO; Grant no. G.0383.16N) and the Excellence of Science program of the Fund for Scientific Research (FWO-FNRS; Grant no. G0F9618N; EOS ID: 30505023). The calculations were performed using the Turing HPC infrastructure at the CalcUA core facility of the Universiteit Antwerpen (UAntwerpen), a division of the Flemish Supercomputer Center VSC, funded by the Hercules Foundation, the Flemish Government (department EWI) and the UAntwerpen. Finally, we also want to thank Dr. Ramses Snoeckx for the very interesting discussions, and A. Fridman and A. Rabinovich for developing the GAP.

Appendix A. Supplementary data

Supplementary material related to this article can be found, in the online version, at doi:https://doi.org/10.1016/j.jcou.2019.05.015.

References

[1] I. Adamovich, S.D. Baalrud, A. Bogaerts, J. Phys. D Appl. Phys. 50 (2017) 323001.
[2] R. Snoeckx, A. Bogaerts, Chem. Soc. Rev. 46 (2017) 5805–5863.
[3] A. Bogaerts, E. Neyts, R. Gijbels, J. van der Mullen, Spectrochim. Acta, Part B 57 (2002) 609–658.
[4] T. Nunnally, K. Gutsol, A. Rabinovich, A. Fridman, A. Gutsol, A. Kemoun, J. Phys. D Appl. Phys. 44 (2011) 274009.
[5] M. Ramakers, G. Trenchev, S. Heijkers, W. Wang, A. Bogaerts, ChemSusChem 10 (2017) 2642–2652.
[6] O. Mutaf-Yardimci, A.V. Saveliev, Aa. Fridman, La. Kennedy, J. Appl. Phys. 87 (2000) 1632.
[7] A. Czernichowski, H. Nassar, A. Ranaivosoloarimanana, A.A. Fridman, M. Simek, K. Musiol, E. Pawelec, L. Dittrichova, Acta Phys. Pol. A 89 (1996) 595–603.
[8] J. Zhu, A. Ehn, J. Gao, C. Kong, M. Aldén, M. Salewski, F. Leipold, Y. Kusano, Z. Li, Opt. Express 25 (2017) 20243.
[9] F. Richard, J.M. Cormier, S. Pellerin, J. Chapelle, J. Appl. Phys. 79 (1996) 2245.
[10] J. Zhu, J. Gao, A. Ehn, M. Aldén, Z. Li, D. Moseev, Y. Kusano, M. Salewski, A. Alpers, P. Gritzmann, M. Schwenk, Appl. Phys. Lett. 106 (2015) 044101.
[11] E. Cleiren, S. Heijkers, M. Ramakers, A. Bogaerts, ChemSusChem 10 (2017) 4025–4036.
[12] J.L. Liu, H.W. Park, W.J. Chung, D.W. Park, Plasma Chem. Plasma Process. 36 (2015) 437–449.
[13] F. Zhu, H. Zhang, X. Yan, J. Yan, M. Ni, X. Li, X. Tu, Fuel 199 (2017) 430–437.
[14] A. Wu, J. Yan, H. Zhang, M. Zhang, C. Du, X. Li, Int. J. Hydrogen Energy 39 (2014) 17656–17670.
[15] X. Tu, J.C. Whitehead, Int. J. Hydrogen Energy 39 (2014) 9658–9669.
[16] A. Indarto, D.R. Yang, J.W. Choi, H. Lee, H.K. Song, J. Hazard. Mater. 146 (2007) 309–315.
[17] J.L. Liu, H.W. Park, W.J. Chung, W.S. Ahn, D.W. Park, Chem. Eng. J. 285 (2016) 243–251.
[18] K. Li, J.L. Liu, X.S. Li, X. Zhu, A.M. Zhu, Chem. Eng. J. 288 (2016) 671–679.
[19] C.S. Kalra, Y.I. Cho, A. Gutsol, A. Fridman, T.S. Rufael, Rev. Sci. Instrum. 76 (2005) 1–7.
[20] L. Bromberg, D.R. Cohn, A. Rabinovich, J.E. Surma, J. Virden, Int. J. Hydrogen Energy 24 (1999) 341–350.
[21] A. Jess, P. Kaiser, C. Kern, R. Unde, C. Von Olshausen, Chemie-Ingenieur-Technik 83 (2011) 1777–1791.
[22] M. Aresta, A. Dibenedetto, A. Angelini, Chem. Rev. 114 (2014) 1709–1742.
[23] B.S. Patil, Q. Wang, V. Hessel, J. Lang, Catal. Today 256 (2015) 49–66.
[24] W. Wang, B. Patil, S. Heijkers, V. Hessel, A. Bogaerts, ChemSusChem 10 (2017) 2145–2157.
[25] A. Bogaerts, E.C. Neyts, ACS Energy Lett. 3 (2018) 1013–1027.
[26] S. Heijkers, R. Snoeckx, T. Kozák, T. Silva, T. Godfroid, N. Britun, R. Snyders, A. Bogaerts, J. Phys. Chem. C 119 (2015) 12815–12828.
[27] T. Silva, N. Britun, T. Godfroid, R. Snyders, Plasma Sources Sci. Technol. 23 (2014) 025009.
[28] R. Snoeckx, S. Heijkers, K. Van Wesenbeeck, S. Lenaerts, A. Bogaerts, Energy Environ. Sci. 9 (2016) 30–39.
[29] S. Heijkers, A. Bogaerts, J. Phys. Chem. C 121 (2017) 22644–22655.
[30] L.F. Spencer, A.D. Gallimore, Plasma Sources Sci. Technol. 22 (2013) 015019.
[31] A. Fridman, Plasma Chemistry, Cambridge University Press, New York, 2008.
[32] B. S. Patil, 2017.
[33] B.S. Patil, F.J.J. Peeters, J.A. Medrano, F. Gallucci, W. Wang, A. Bogaerts, Q. Wang, G. Van Rooij, J. Lang, V. Hessel, Appl. Energy (2018) Submitted.
[34] Z. Bo, J. Yan, X. Li, Y. Chi, K. Cen, J. Hazard. Mater. 166 (2009) 1210–1216.
[35] A. Evans, R. Luebke, C. Petit, J. Mater. Chem. A Mater. Energy Sustain. 6 (2018) 10570–10594.
[36] T. Namihira, S. Katsuki, R. Hackam, H. Akiyama, K. Okamoto, IEEE Trans. Plasma Sci. IEEE Nucl. Plasma Sci. Soc. 30 (2002) 1993–1998.
[37] J.F. Coudert, J.M. Baronnet, J. Rakowitz, P. Fauchais, Synthesis of Nitrogen Oxides in a Plasma Produced by a Jet Arc Generator, (1977).
[38] M. Rahman, V. Cooray, Opt. Laser Technol. 35 (2003) 543–546.
[39] W. Bian, X. Song, J. Shi, X. Yin, J. Electrost. 70 (2012) 317–326.
[40] N. Rehbein, V. Cooray, J. Electrost. 51 – 52 (2001) 333–339.
[41] V.M. Shmelev, A.V. Saveliev, L.A. Kennedy, Plasma Chem. Plasma Process. 29 (2009) 275–290.
[42] B.S. Patil, N. Cherkasov, J. Lang, A.O. Ibhadon, V. Hessel, Q. Wang, Appl. Catal. B 194 (2016) 123–133.
[43] B. Mutel, O. Dessaux, P. Goudmand, Agressologie 19 (1984) 461–464.
[44] L.S. Polak, A.A. Ovsiannikov, D.I. Slovetsky, F.B. Vurzel, Theoretical and Applied Plasma Chemistry, Nauka (Science), Moscow (1975).
[45] R.I. Asisov, V.K. Givotov, V.D. Rusanov, A. Fridman, Sov. Phys. High Energy Chem. (Khimia Vysok. Energy 14 (1980) 366.
[46] T. Kim, S. Song, J. Kim, R. Iwasaki, J. Appl. Phys. 49 (2010) 126201.
[47] M.A. Malik, C. Jiang, R. Heller, J. Lane, D. Hughes, K.H. Schoenbach, Chem. Eng. J. 283 (2016) 631–638.
[48] K. Birkeland, Trans. Faraday Soc. 2 (1906) 98–116.
[49] J. Krop, I. Pollo, Chemia 678 (1981) 51–59.
[50] R. Ingels, D. Graves, S. Anderson, R. Koller, Int. Fertil. Soc. Conf. (2015) 1–27.
[51] G. Trenchev, S. Kolev, W. Wang, M. Ramakers, A. Bogaerts, J. Phys. Chem. C 121 (2017) 24470–24479.
[52] J.G. Chen, R.M. Crooks, L.C. Seefeldt, K.L. Bren, R. Morris Bullock, M.Y. Darensbourg, P.L. Holland, B. Hoffman, M.J. Janik, A.K. Jones, M.G. Kanatzidis, P. King, K.M. Lancaster, S.V. Lymar, P. Pfromm, W.F. Schneider, R.R. Schrock, Science (80-.). 360 (2018).
[53] L. Wang, M. Xia, H. Wang, K. Huang, C. Qian, C.T. Maravelias, G.A. Ozin, Joule 2 (2018) 1055–1074.
[54] R. Lan, K.A. Alkhazmi, I.A. Amar, S. Tao, Appl. Catal. B Environ. 152–153 (2015) 212–217.
[55] P. Peng, P. Chen, C. Schiappacasse, N. Zhou, E. Anderson, D. Chen, J. Liu, Y. Cheng, R. Hatzenbeller, M. Addy, Y. Zhang, Y. Liu, R. Ruan, J. Clean. Prod. 177 (2018) 597–609.
[56] A.J. Martín, T. Shinagawa, J. Pérez-Ramírez, Chem (2018), https://doi.org/10.1016/j.chempr.2018.10.010.
[57] N. Cherkasov, A.O. Ibhadon, P. Fitzpatrick, Chem. Eng. Process. Process Intensif. 90 (2015) 24–33.
[58] T. Kozák, A. Bogaerts, Plasma Sources Sci. Technol. 23 (2014) 045004.
[59] A. Bogaerts, T. Kozák, K. van Laer, R. Snoeckx, Faraday Discuss. 183 (2015) 217–232.
[60] A. Berthelot, A. Bogaerts, Plasma Sources Sci. Technol. 25 (2016) 045022.
[61] A. Ozkan, T. Dufour, T. Silva, N. Britun, R. Snyders, A. Bogaerts, F. Reniers, Plasma Sources Sci. Technol. 25 (2016).